Accepted Manuscript

An ultrasensitive label free human papilloma virus DNA biosensor using gold nanotubes based on nanoporous polycarbonate in electrical alignment

Mohsen Shariati, Mohammad Ghorbani, Pezhman Sasanpour, Ali Karimizefreh

PII: S0003-2670(18)31166-8

DOI: 10.1016/j.aca.2018.09.062

Reference: ACA 236298

To appear in: *Analytica Chimica Acta*

Received Date: 1 May 2018

Revised Date: 16 September 2018

Accepted Date: 26 September 2018

Please cite this article as: M. Shariati, M. Ghorbani, P. Sasanpour, A. Karimizefreh, An ultrasensitive label free human papilloma virus DNA biosensor using gold nanotubes based on nanoporous polycarbonate in electrical alignment, *Analytica Chimica Acta* (2018), doi: https://doi.org/10.1016/j.aca.2018.09.062.

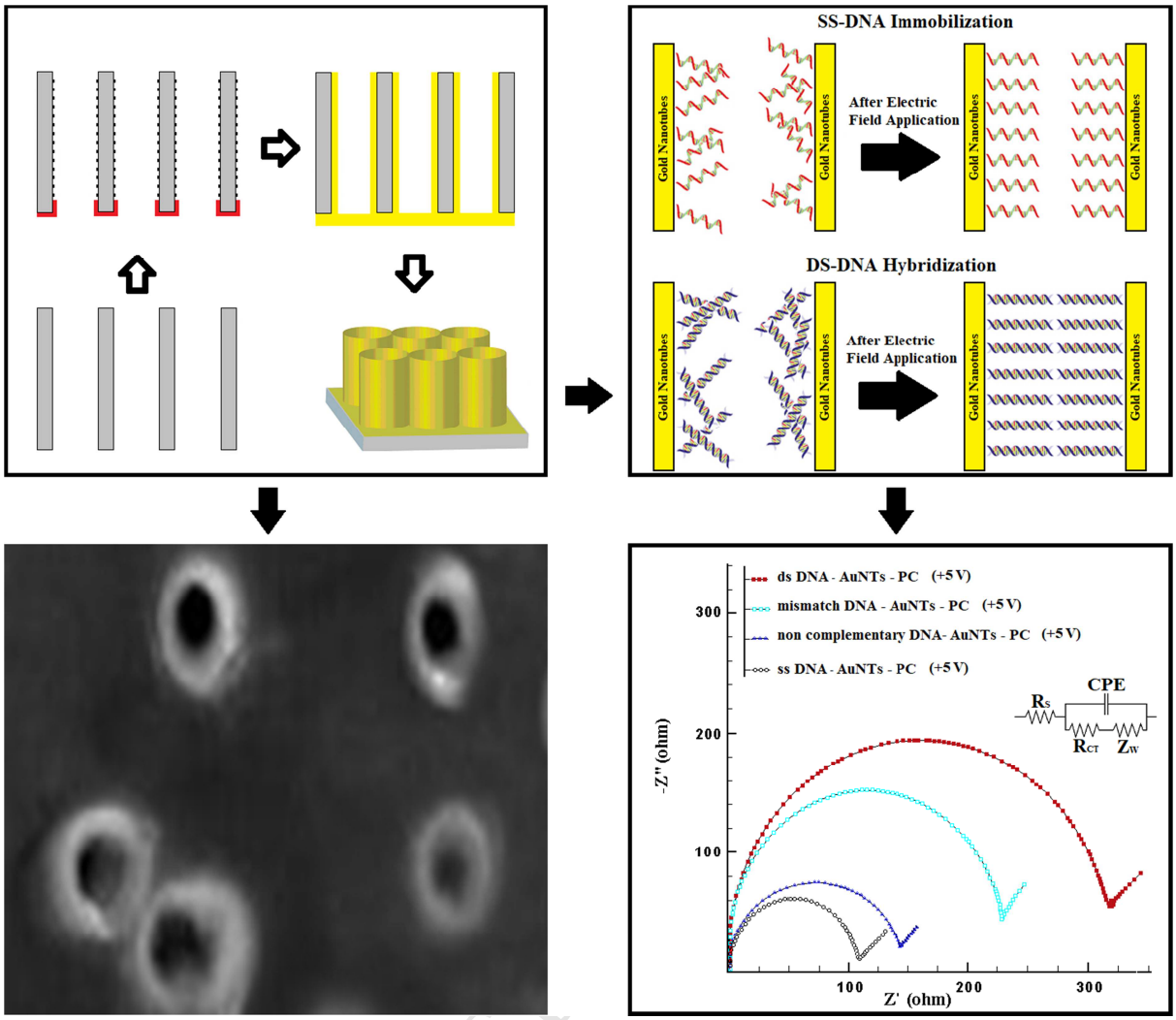

An ultrasensitive label free human papilloma virus DNA biosensor using gold nanotubes based on nanoporous polycarbonate in electrical alignment

Mohsen Shariati[a], Mohammad Ghorbani[a,b]*, Pezhman Sasanpour[c], Ali Karimizefreh[c]

[a] Institute for Nanoscience and Nanotechnology, Sharif University of Technology, P.O. Box 11155-8639, Tehran, Iran
[b] Department of Materials Science and Engineering, Sharif University of Technology, P.O. Box 11155-9466, Tehran, Iran
[c] Department of Medical Physics and Biomedical Engineering, School of Medicine, Shahid Beheshti University of Medical Sciences, Tehran, Iran

*Corresponding author at: P.O. Box 11155-8639, Tehran, Iran. Tel.: +98 2166165219; fax: +98 2166005717.
E-mail addresses: Ghorbani@sharif.edu (M. Ghorbani)

Abstract: An impedimetric human papilloma virus (HPV) DNA biosensor based on gold nanotubes (AuNTs) in label free detection was materialized. The AuNTs decorated nanoporous polycarbonate (AuNTs-PC) template as biosensor electrode was fabricated by electrodeposition method. The single strand DNA (ss-DNA) probe was covalently immobilized onto the AuNTs-PC electrode. The hybridization of target sequences with the ss-DNA probe was observed by the electrochemical impedance spectroscopy (EIS). The biosensor showed high selectivity and could differentiate between the complementary, mismatch and non-complementary DNA sequences. The EIS measurements were matched to Randle's equivalent circuit. The negatively-charged HPV DNA oligonucleotides under external electric field were oriented in a preferred direction and the bio-sensing responses were intensified by controlling the immobilization and hybridization of the sequences on the AuNTs surface. The fabricated DNA biosensor under electric field amplification was stable up to six weeks and demonstrated 97% of its initial detection responses. The biosensor displayed the HPV DNA hybridization detection in very low concentrations in the linear response ranges of 0.01 pM to 1 μM and was able to acquire a limit of detection (LOD) of 1 fM.

Keywords: Human Papilloma Virus DNA; Nanoporous polycarbonate; Gold Nanotubes; Electrochemical Impedance Spectroscopy; Biosensor.

1. Introduction

Human papilloma virus infection is a type of human papilloma virus (HPV), [1]. Most of the human papilloma virus infections are symptom-free and not resolved automatically, [1-4]. In some patients, the human papilloma virus infection causes warts or pre-cancerous ulcers, [1]. There are three classified categories, comprising about 200 types of papilloma viruses, depending on their role in the development of cervical cancer, they are denominated as low-risk, moderate and high-risk categories [2-7]. The high risk genetic species of the HPV has a significant role in the engenderment of cervical cancer, and this is the third most common cancer in the post-endometrial women and ovarian cancer in the United States, [2]. The cancer resulted by HPV infection is one of the leading inducements of fatality worldwide and is the second leading cause of cancer depravity among women in developing countries, [2, and 7]. Among the 14 known high-risk species of the human papilloma viruses, two of them, subspecies HPV16 and HPV18 are the most important high-risk genotypes around the world and they have been monitored in 62% of cases related to cervical cancer. About 93% of the cervix related cancers can be prevented, thus their diagnosis and recognition are extremely vital, [2]. Due to its low sensitivity and specificity, the detection of the HPV via

cell culture and serological testing may not be easily detected achievable, [2-4]. In contrast, molecular cervical cancer screening techniques including hybrid capture assay tests and polymerase chain reaction (PCR) are the efficient techniques for the detection of HPV, [4]. However, the mentioned techniques are basically dependent on the DNA sensing of viruses. However, the preparation and purification of samples in the mentioned techniques are very challenging and excessively time consuming.

Electrochemical impedance spectroscopy (EIS) detection is one of the most promising mechanisms in label free bio-sensing especially in DNA detection, [2, 8-9]. The EIS measurement studies the dielectric parameters of a biological system in wide frequencies, [9-12]. The EIS has demonstrated to provide information on wide basic processes such as surface adsorption, charge transfer, ion exchange and diffusion, [9-13]. The EIS provides the fundamental and functional information at the interface between the electrode and electrolyte, [9-11]. The electrochemical impedance measurement system as a non-destructive and relatively facile to use detection system has been widely used in the field of label-free biosensors that are sensitive to cell culture monitoring, interaction between antibody and antigen [9-15], and DNA oligonucleotides hybridization, [10-13]. The evolution of the precise and highly sensitive impedance biosensors using nanostructures materials has occupied many interests in the past few years, [2, 11-15]. Recently, the arrays of the Au nanotubes have been very attractive due to their significant characteristics, such as high sensitivity in the detection of complex materials, especially their physicochemical stability, [16]. The Au nanotubes were used effectively as sensitive electrode for amperometric bio-sensing, [17]. In order to sense the mycobacterium tuberculosis DNA, an electrochemical biosensor based on Au nanotubes platform was fabricated, [18]. The highly sensitive dodecanethiolate based Au nanotubes electrode was applied for mercury detection, [19]. The bio-functionalized Au nanotubes for protein detection were materialized conically, [20]. The Au nanotubes-based PC biosensor was also used for ultrasensitive DNA detection, [21]. The plasmonic Au nanotubes indicated high-performance in bio-sensing, [22]. Due to the high sensing characteristic of Au nanotubes to detect the biological materials and DNA, several scientific techniques have been proposed for fabrication of short and long Au nanotubes in polycarbonate templates by electroless and electrochemical mechanism, [23-25].

Recently some useful and practical techniques have been used to enhance the DNA sensing, [26-28]. One of the best techniques is the applying of electric filed for improving the hybridization on the surface and promoting the sensing ability. The rate of hybridization of DNA targets to immobilized probes has been studied with the electric field, recently, [26]. By applying the external electric field, the hybridization time of the DNA targets with probe, depending on target size, was decreased from 10-30 hrs to 10-60 min, [26]. By applying the external electric field, probes and targets orientate flat on the surface. The electric field enhanced hybrid capture of solution-phase targets by surface-bound probes, [26]. A simulated model discusses the kinetics measured and also involves surface states between initial target arrival and final hybridized state, [26]. A clamped homogeneous electrical field electrophoresis (CHEF) was used to study the biological effects of electric and magnetic fields (EMFs), [27]. This CHEF authorizes the separation of DNA sequences in presence of the electric and magnetic fields, [27]. In comparison to the optical trapping, the DNA oligonucleotides can be materialized in aqueous solution. Due to the induction of an electric dipole, DNA molecules are pulled by a gradient force to regions of high electric field strength, [27]. By mixing static and oscillating electric fields, trapped molecules can be propelled from one edge to another or made to follow precise trajectories along the edges, [28].

In this paper, the HPV16 DNA biosensor based on AuNTs under external electric field bias is presented. The AuNTs-PC template was used as biosensor electrode. The AuNTs-PC template electrode was fabricated by the electrodeposition mechanism. The EIS measurements and electrochemical responses of the HPV DNA biosensor were investigated. After materialization of the AuNTs surface, the immobilization and hybridization process of the HPV16 DNA oligonucleotides were studied. The AuNTs-PC electrode under electric field improved the surface coverage, the sensitivity of detection and selectivity of the biosensor. In this scientific approach, the rapid, stable and reproducible biosensor of the HPV16 DNA was achieved. For comparison the bare PC template was also involved in DNA bio-sensing investigation.

2. Experimental section

2.1. Materials

Potassium chloride, $K_4Fe(CN)_6$, $K_3Fe(CN)_6$, ethanol, HCl, NaCl, EDTA (Ethylenediaminetetraacetic acid), and $Na_3C_6H_5O_7$ were purchased from Merck. The PC template was obtained from Whatman Co. the Phosphate buffer saline (PBS), Dithiothreitol (D.T.T), $NiSO_4 \cdot 6H_2O$, H_3BO_3, $KAu(CN)_2$, CH_2Cl_2, 3-aminopropyltriethoxysilane (APES), PVP (polyvinylpyrrolidone) were prepared from Sigma Aldrich.

The buffers used in this work were as follows: DNA immobilization buffer: buffer Tris-EDTA (TE, 10 mM Tris–HCl, 1 mM EDTA, pH 8.0), hybridization buffer: 2× saline sodium citrate (SSC, 300 mM NaCl, 20 mM $Na_3C_6H_5O_7$, pH 7.0). Electrolyte solution was 0.2 M KCl solution containing 2 mM $K_4Fe(CN)_6/K_3Fe(CN)_6$ (1:1). All solutions were prepared in deionized water (DI water). 25-mer ss-DNA sequence with HS-$(CH_2)_6$-modification at the 5′-end with HPLC purification (as HPV 16 probe) and all target oligonucleotides with BIO-RP purification were provided. Stock solutions (100 μM) of the DNA sequences were prepared with sterile distilled water (SD water) and stored at a refrigerator at −20 °C. Specificity of the oligonucleotide sequences were investigated with Basic Local Alignment Search Tool (BLAST) [21]. The used oligonucleotides sequences were listed in table 1.

Table 1. The HPV16 DNA oligonucleotides sequences

Sequence name	Sequence of oligonucleotides	Company (Country)
Thiolated-probe	5′ - SH-AAAGCAAAGTCATATACCTCACGTC - 3′	Bioneer Corporation (South Korea)
Complementary	5′ - GACGTGAGGTATATGACTTTGCTTT- 3′	Bioneer Corporation (South Korea)
One-point Mismatch	5′ - ACG CCA GAT GAA GAA GGG GAC GGT A - 3′	Bioneer Corporation (South Korea)
Non-complementary	5′ - AACGTGAGGTATATGACTTTGCTTT- 3′	Bioneer Corporation (South Korea)

2.2. AuNTs fabrication in the PC pores

The electrodeposition process for the fabrication of AuNTs inside the PC template pores were performed in three-electrode electrochemical cell using an instrumental potentiostat measurement (Autolab, PGSTAT302N). Fig. 1 schematically shows the electrodeposition process for AuNTs fabrication. The Ag/AgCl electrode and platinum wire were used as the reference and counter electrode, respectively. The PC template in the biosensor materialization approach was used as template and the size of the pores was around 150-200nm. The hydrophilic inner side of the pores was coated with PVP (polyvinylpyrrolidone). In order to functionalize the inside of the pores, all the PC templates were ultrasonically exposed to the 3-aminopropyltriethoxysilane (APES) for 35 min. Also, APES can be utilized as a coupling agent. Therefore, APES molecules activated and functionalized the inside of the pores. Due to well absorption of the ethoxy groups of the APES molecules to hydrophilic walls of the pores, Au ions will be strongly adsorbed on amino groups and Au nanostructures could grow vertically rather than radially, [23]. To ensure a good electrical contact, a thin layer of Au with the thickness of 20 nm was sputtered on one side of the template. This layer is too thin to bridge over the pores and leaves the pores open. Then the PC template ultrasonically was cleansed in the DIW for 10 min. The sputtered side of the template was attached to the working electrode and the bare side was exposed to the solution. Before the fabrication of AuNTs in the cell, first, nickel was

electrodeposited. The electrodepositing process was performed at −900 mV (fixed potential) in the solution (0.8 mol/L $NiSO_4 \cdot 6H_2O$, 0.5 mol/L H_3BO_3, 0.3 mol/L KCl in 1 min). This process was led to the fabrication of the short nickel nanotubes, which maintain the backside of the PC (sputtered with Au) from dissolution in electrodepositing process. It has been known that for electrodepositing of the ions inside the pores rather than lateral deposition, the high negative voltage is required, [25]. The nickel nanotubes were electrodeposited at the end of the pores and they facilitated the deposition of the Au ions inside of the pores. In order to fabricate the AuNTs, the electrodeposition process was performed in the potassium gold cyanide (10 mM $KAu(CN)_2$) at −1400 mV for 300 s. After the fabrication of AuNTs, the PC template was washed and cleansed in DI water and then partially dissolved in CH_2Cl_2 by adding a few drops of CH_2Cl_2 on PC template for 15 min.

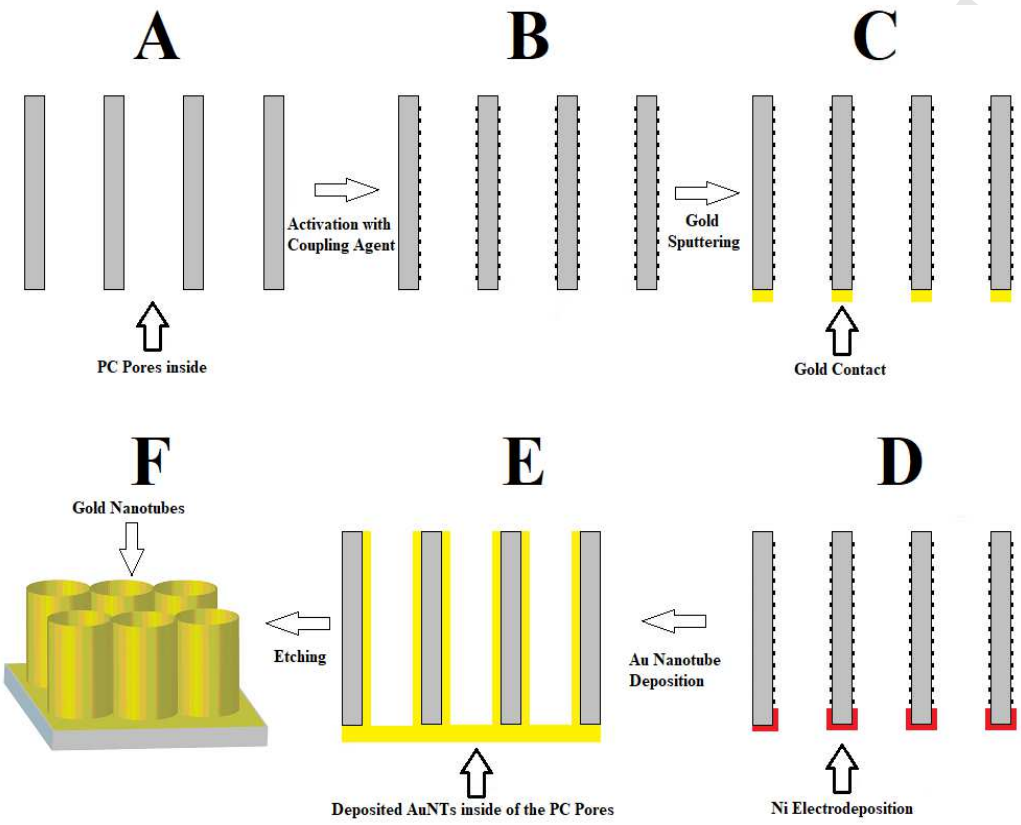

Fig. 1. The schematic illustration of the AuNTs synthesis. (A) The PC and the pores inside. (B) The modification of the pore walls with molecular anchor. (C) For better contact materialization, an Au thin film was sputtered on one face of the PC. (D) The electrodeposition of nickel nanotubes. (E) The elecrodeposition of the AuNTs. (F) The preparation AuNTs after PC template etching.

2.3. DNA immobilization and hybridization processes on the AuNTs surface

In order to immobilize the ss-DNA probe on both the AuNTs-PC surface and typical bare PC surface, first the ss-DNA probes were inserted in D.T.T solution diluted in PBS (pH~8.2) in 0.1 M concentration for 20 min to separate the disulfide bond of the probes. For immobilization, 1 µL of the thiol-modified sequences (1 µM concentration) in TE buffer (10 mM Tris–HCl, 1 mM EDTA, pH 8.0) were drop-casted on the surface of the electrode and then the electrode was maintained in a sealed box to inhibit contamination and preserve the disposed materials on the PC template surface, see the schematic illustration in Fig. 2. The sample was kept at room temperature around 6 hrs and then washed carefully with DIW (deionized water). For hybridization with the target sequences, 1 µL of target sequences volume (different concentrations from 1 µM to 0.01 pM for sensitivity) in SSC buffer (pH ~7.0) was exposed to the surface of the probe-modified PC and AuNTs-PC electrode, and the electrodes were maintained in the sealed box. Finally the samples were washed and rinsed by SSC and the EIS measurements were materialized.

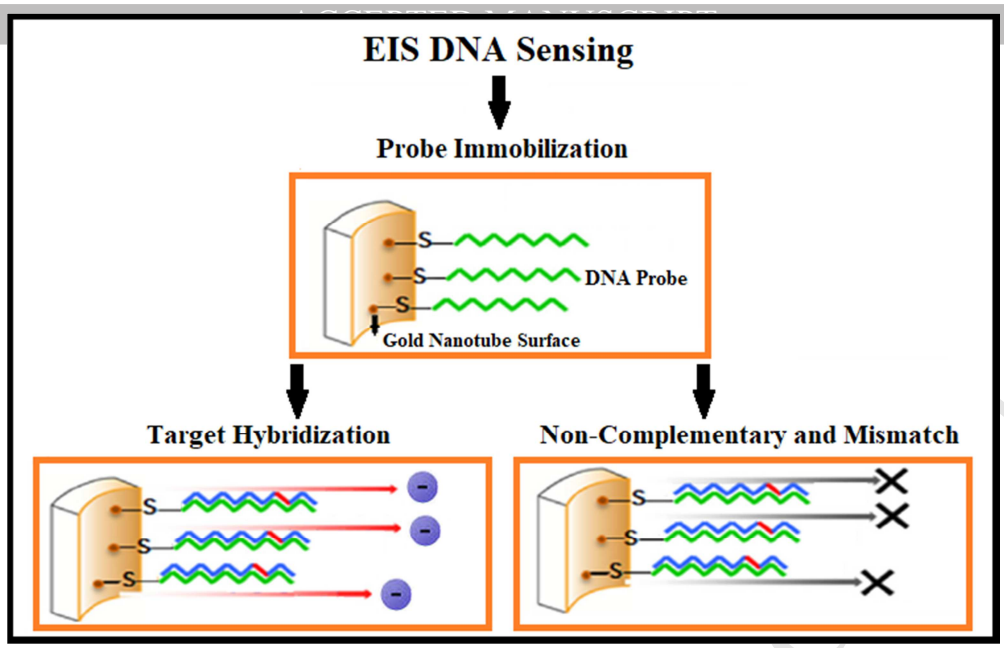

Fig. 2. The modifications of the AuNTs surface. The schematic image for probe immobilization and hybridization of the HPV DNA target sequences on the AuNTs PC surface.

2.4. Structural and morphological characterization of the AuNTs-PC

The field emission scanning electron microscope (FESEM) (Hitachi model: S-4160) was used to characterize the morphology of the AuNTs-PC and to demonstrate a prospective illustration of AuNTs. A transmission electron microscopy (TEM) (model; Philips, CM-30) was utilized for determining the DNA attachment on the surface of the AuNTs, their size and directional alignment.

2.5. The EIS measurements of the DNA biosensor

The electrochemical impedance spectroscopy measurements were performed by using a frequency response analyzer and Autolab PG STAT302N potentiostat with a conventional three-electrode test cell utilizing Ag/AgCl as reference and platinum as counter electrodes. The EIS measurements were conducted with the FRA32M module. Electrolyte solution was 0.2 M KCl solution containing 2 mM $K_4Fe(CN)_6/K_3Fe(CN)_6$ (1:1). All solutions were prepared in deionized water (DI water). All impedance spectra were taken using ac modulation of +10 mV over the frequency range from 0.01 Hz to 100 KHz without dc bias with respect to open circuit potential. In order to optimize the capabilities of the HPV16 DNA biosensor, the AuNTs-PC electrode was subjected to a potential driving force. The electrical field was applied from +5 V to +40 V. In order to confirm the EIS measurements, all experiments were performed 3 times and conducted at room temperature. The schematic illustration of the bio-sensing system under electric field amplification is demonstrated in Fig. S1.

3. Results and discussion

3.1. Morphological FESEM, EDX and HRTEM characterizations

The morphological FESEM characterizations of the fabricated AuNTs have been displayed in Fig. 3. It is obviously observed that the AuNTs have been fabricated inside the PC template pores. Fig. 3A and B are top surface images of the PC template at the start and the end of AuNTs elctrodeposition decoration process, respectively. Slow kinetic, indeed, was essential for the AuNTs fabrication. The cross section image

of the PC template at initial steps has been demonstrated in Fig. 3C. Fig. 3C also indicates the Au nanoparticles inside of the PC pores in elctrodeposition process after 50 s. In this stage, Au nanoparticles clearly materialized the nucleation sites inside the pores. Fig. 3D demonstrates the cross section image of the PC template at the end of the growth process. Fig. 3D indicates Au deposition inside the PC template. In Fig. 3E and F, the top view picture of the AuNTs-PC template is presented. In Fig. 3E, the fabricated AuNTs inside the PC template pores are obviously observed. The size of the edge side of the AuNTs is around 30-50 nm, Fig .3F. The average diameter of the AuNTs is around 100 nm. It is obviously seen a large quantity of AuNTs have been grown inside the PC template. The AuNTs intensively amplified the EIS measurements for bio-sensing under external electric field bias.

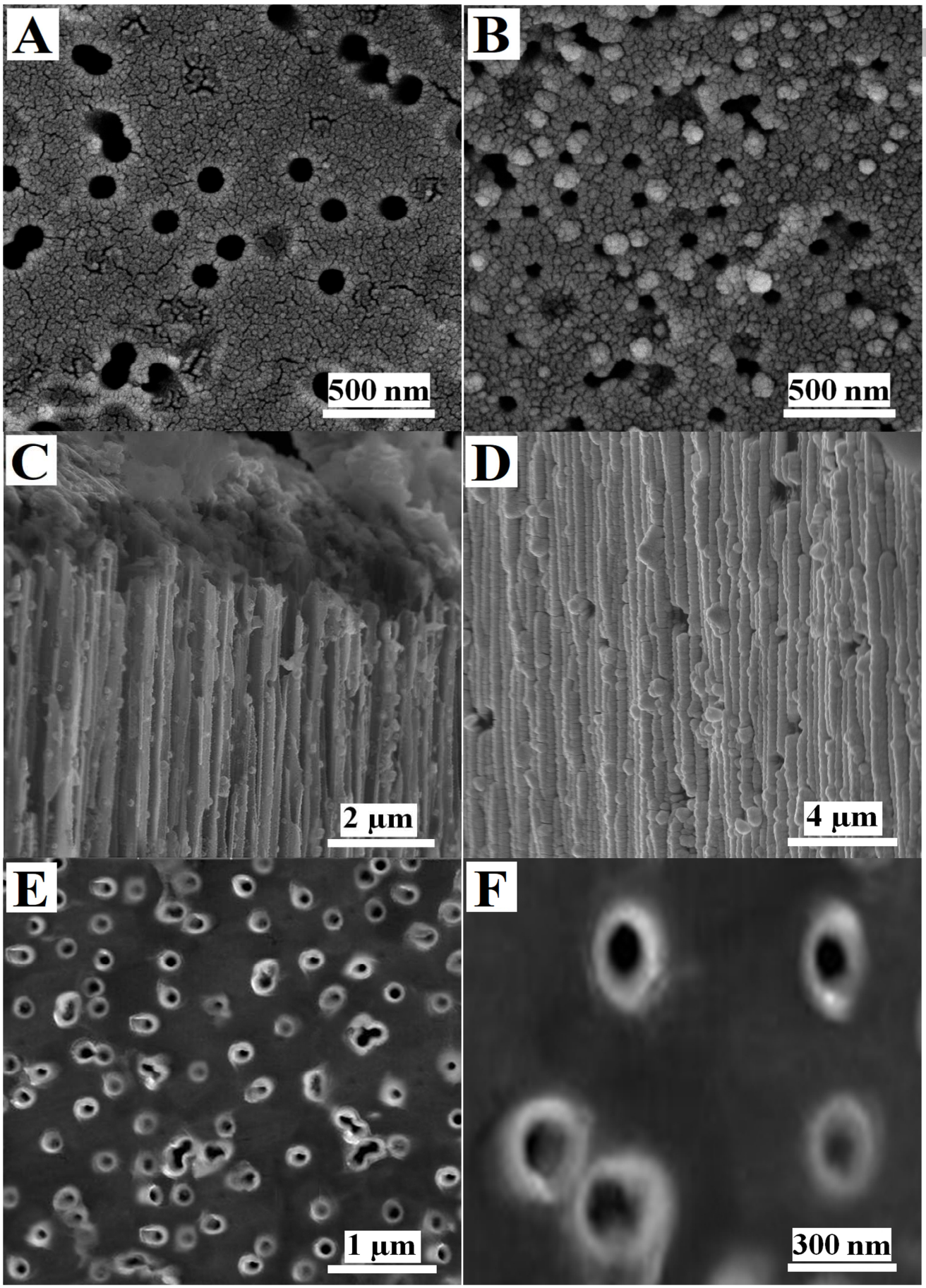

Fig. 3. The FESEM images of the AuNTs-PC template. (A) The surface of the PC template at the start of the Au decoration, top view. (B) The surface of the PC template at the end of the Au decoration, top view. (C) The Au nanoparticles inside of the PC pores, cross section image after 50 s electrodeposition process. (D) The cross section image of the PC template at the end of the

electrodeposition process. (E) The AuNTs, at the end of fabrication process. (F) The AuNTs (in final stage) fabricated in under controlled synthesis inside the pores, magnified resolution.

In order to detect the elements presence in the AuNTs-PC electrode, the EDX-mapping for atomic elements characterization was performed (characterization from cross sectional parts). Fig. 4 shows the EDX-mapping. Fig. 4A and B validate the carbon and oxygen. Fig. 4C and D indicate the volume and distribution scheme of the oligonucleotides and Au in the AuNTs-PC electrode. The EDX-mapping measurements of the oligonucleotides and Au proved the DNA and AuNTs presence in the electrode. The detection of phosphorus (P, phosphate backbone of DNA) on the surface and their randomly distribution were validated by the EDX elemental map.

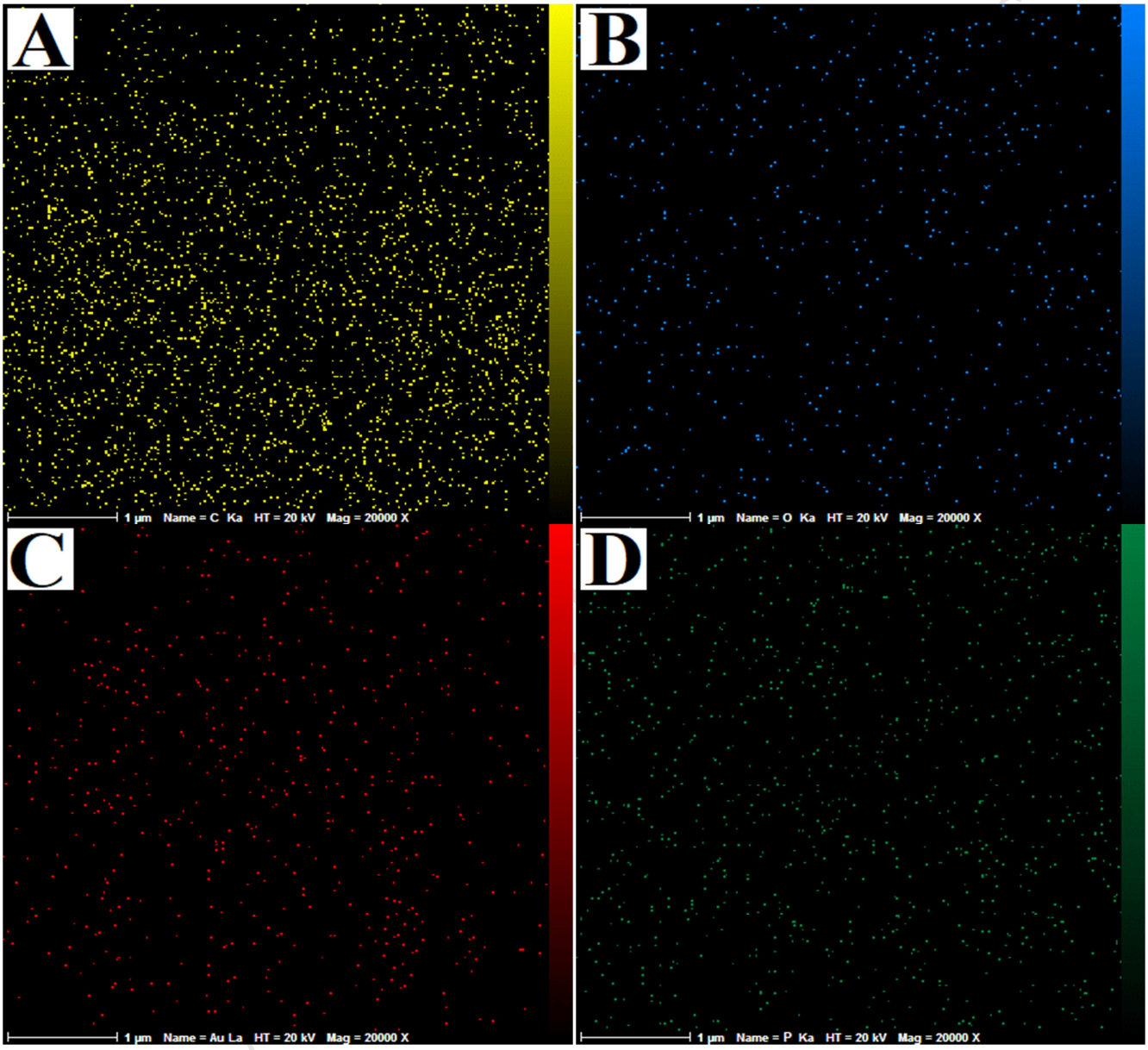

Fig. 4. The EDX-mapping for atomic elements detection; (A) Carbon, C; (B) Oxygen, O; (C) Gold, Au; (D) Phosphorus, P; on the cross section surface of the AuNTs-PC (inside the pores). The characterized validation of the P and Au presence for verifying Au and DNA attachments.

The size and detailed morphology of the DNA sequences and their attachment to the surface of the AuNTs after electric field amplification were investigated by the high resolution transmission electron microscopy (HRTEM) analysis. The corresponding high resolution TEM image of the selected DNA sequences is illustrated in Fig. 5. The HRTEM image of DNA sequences demonstrates that they are around 5 nm in size. Fig. 5 demonstrates that the oligonucleotides were aligned under electric potential. Inset validates the alignment of the helical oligonucleotides. Inset shows helical shape of DNA sequences in

magnified resolution. In Fig. 5 the attachment of the DNA sequences to the AuNTs surface is clearly validated.

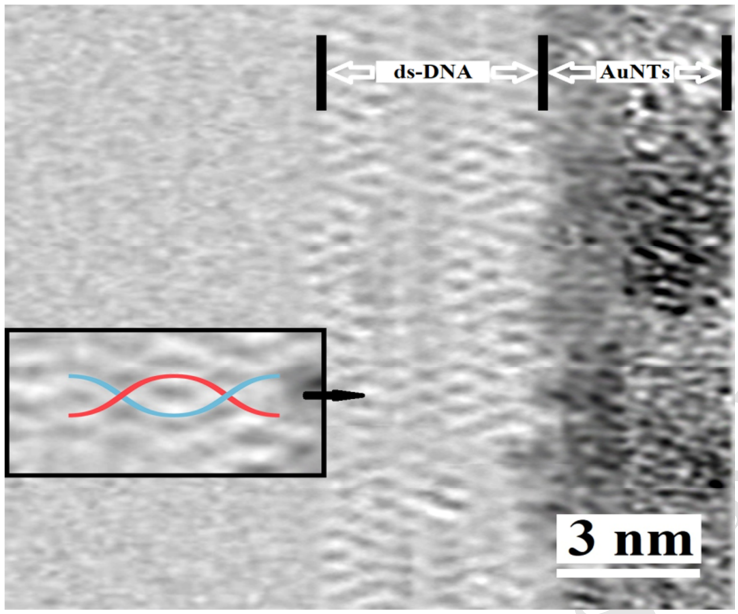

Fig. 5. The HRTEM image of AuNT associated with DNA sample after applying the electric field. The DNA sequences in the edge of AuNT. The alignment of the DNA sequences after applying the electric field. Inset; the helical shape of DNA sequences in magnified resolution.

3.2. The Electrochemical DNA biosensor characterization

The electrochemical DNA biosensors intensively rely on the immobilization and hybridization of the DNA probe and target oligonucleotides on the sensor electrode surface. The 3-D nanostructured-based materials electrodes are the most capable to be used in the electrochemical sensing of the DNA, [10, 29-31]. The 3-D nanostructured-based templates have well-defined micro-fluidic channel structures which provide satisfying design templates for DNA sensing. In comparison to one-dimensional (1-D) probe DNA electrodes, 3-D nanostructured-based materials electrodes such as PC could fix the distribution limits, packing density restrictions and sensitivity problems, [30, 31]. Due to the high surface-to-volume ratio and extreme sensitivity to target molecules, Au decorated PC template has been significant candidates for DNA sensing, [30, and 31]. These materials would resolve diffusion resistance in sensing process. After immobilization process, due to the interaction of the ions on the AuNTs-PC electrode surface, electrostatic repulsion would cause R_{ct} enhancement. At the electrolyte/electrode interface, negative charges can be repulsed from the surface and positive charges can align along the AuNTs surface due to the higher concentration of the positive charges in comparison to the negative charges. This process can cause challenges in the transfer of the charges, forming an interfacial layer and ultimately increase the resistance, [29].

3.2.1. The EIS selectivity studies of the PC and AuNTs-PC (with and without electric potential) electrodes

In order to measure the specificity and selectivity of the fabricated DNA biosensor, the investigation of the hybridization of the mismatch, non-complementary and complementary DNA oligonucleotides with the probe (ss-DNA) was conducted. The specificity of the biosensor is a crucial capability for measuring its bio-sensing parameters. Fig. 6 shows the EIS measurements for PC and AuNTs-PC (with and without electric potential). Fig. 6A shows the Nyquist plots (EIS spectra using $[Fe(CN)_6]^{3-/4-}$ as redox maker ions), for the bare PC electrode and Fig. 6B and C indicate the Nyquist plots for AuNTs-PC electrode modified

with DNA oligonucleotide without and with electric potential, respectively. Fig. 6D shows the charge transfer resistance (R_{ct}) values for DNA electrodes obtained from EIS measurements. The results have been achieved after three independent different tests for ss-DNA, non-complementary, mismatch and complementary DNA targets. All experiments were measured in 1 µM concentration.

As depicted in Fig. 6A, the R_{ct} was increased by the hybridization of the probe oligonucleotide (ss-DNA) on the electrodes surface and inside the pores with ds-DNA. The semicircle diameter and the linear line in the impedance plot illustrate R_{ct} and the capacitance behavior, respectively. The resistivity enhancement was mainly due to the electrostatic repulsion of the negatively-charged phosphate groups and the dielectric backbone of the DNA, [29]. The corresponding R_{ct} in the bare PC electrode were dropped from 11453 Ω to 11016 Ω for complementary and mismatch targets after hybridization with probe, respectively, Fig. 6D. The decreased electrostatic interactions (repulsive interactions) at the interface between electrode and electrolyte were the main factors that influenced the R_{ct} alterations significantly. The charge transfer had been hindered by repulsion through the interface, [1-5]. The probe modified PC electrode indicated the lowest R_{ct}, and the R_{ct} of the functionalized probe surface was 7312 Ω, Fig. 6D. Due to electrostatic and steric repulsion, the probe modified PC electrode demonstrated intensive charge transfer between electrolyte and the electrode surface, in comparison to hybridization measurements. This intensive charge transfer reduced the semicircle diameter of the EIS spectrum diagram, [2-4]. Due to weak complementary duplex materialization between non-complementary DNA oligonucleotides and PC surface, a weak hybridization has been demonstrated in comparison to complementary and mismatch oligonucleotides and the R_{ct} value was around 9125 Ω, Fig. 6D.

Fig. 6B and C show the specificity of the AuNTs-PC electrode surface with ss-DNA, mismatch, non-complementary and complementary oligonucleotides without and with applying electric potential respectively. In Fig. 6B, the EIS impedance spectra were investigated for the AuNTs-PC electrode modified with ss-DNA probe, and their hybridization bio-sensing without electric potential amplification. As shown in Fig. 6B, the diameters of the electrochemical impedance semi-circles of the AuNTs-PC were critically reduced in comparison to the bare PC electrode, because of the AuNTs accommodation. In Fig. 6B the results indicate that the AuNTs-accommodated electrode proved to possess a significant ability in DNA sensing. The corresponding R_{ct} were reduced from 1226 Ω to 472 Ω for ds-DNA AuNTs-PC electrode and ss-DNA AuNTs-PC electrode respectively, Fig. 6D. The repulsive forces caused from phosphate groups were the main factors for higher R_{ct}, [29]. The semi-circle diameter value of the probe hybridization with complementary target was increased in comparison to non-complementary hybridization. This means that the R_{ct} was increased by the formation of the complementary duplex and the change was around ΔR_{ct} = 685 Ω, Fig. 6D. Due to the electrostatic repulsive interactions without any nonspecific binding, the EIS measurement under employing non-complementary oligonucleotides represented more charge transfer and decreased resistance. In comparison to the probe, the electrostatic repulsion between the redox marker ions and AuNTs-PC enhanced R_{ct}, Fig. 6D. Fig. 6C shows the specificity of the AuNTs-PC electrode with ss-DNA, mismatch, non-complementary and complementary oligonucleotides with applying electric potential. The corresponding R_{ct} were reduced from 325 Ω to 106 Ω for ds-DNA AuNTs-PC electrode and ss-DNA AuNTs-PC electrode, respectively, Fig. 6D. In this work, AuNTs-PC electrode under electric field amplification was subjected to the HPV16 DNA. The pore diameter and overall density with AuNTs decoration accommodated the DNA sensing. By applying the electric field via establishing a voltage, the sensor could increase the level of DNA immobilization and hybridization to the surface of the electrode and also enhance the stability and minimize the concentration for DNA detection, Fig. S2. An applied electric field will polarize the material by orienting the dipole moments of polar molecules. The presence of the dielectric decreases the electric field produced by a given charge density, Eq. (1).

$$E_{effective} = E_{external} - E_{polarization} \quad (1)$$

This effective electric field ($E_{effective}$) will cause the alignment of the DNA sequences on the surface and enhance the surface coverage and finally increase the response, Fig. 5. By applying the electric field, the charge transfer was increased. This process supports the bio-sensing mechanism at very low concentrations.

The inset in the Fig. 6C demonstrates the Randle's equivalent circuit. In the Randle's circuit, R_{ct}, C_{DL} and R_S are the charge transfer resistance, the double layer capacitor in the interface between electrode and solution and the electrolyte resistance, respectively. In the Randle's equivalent circuit, Warburg impedance (Z_W) originates from the redox couple diffusion and the electrode at low frequencies, [24].

The capability of the AuNTs-PC biosensor was optimized by exploiting the capacitance mechanism of the AuNTs-PC electrode under electrical field bias. The impacts of the applied electrical field on the HPV16 DNA biosensor for ss-DNA and ds-DNA under different potentials in 0.01 pM concentration were investigated. Fig. 6 (E, F) indicate the EIS spectra for the probe modified AuNTs-PC electrode and hybridization with complementary target under electric field amplification. The parameters for the Randle's equivalent electrical circuit elements obtained from the simulation of the impedance spectra of the AuNTs-PC electrode under electric field amplification are indicated in table 2. The EIS measurements were contentedly fitted to the circuit elements. Initially, in this measurement, the effect of the probe immobilization on the AuNTs-PC electrode was checked by the applied potential, Fig. 6E. It is completely seen that as the applied electric field enhanced, R_{ct} in the EIS measurements was reduced. The R_{ct} was reduced from 106 Ω to 26 Ω for +5 V and +40 V, respectively, table 2. Then the response of the target hybridization with probe was investigated, (Fig. 6F). The concentration was fixed in 0.01 pM. As the potential driving force was increased, the resistance and R_{ct} were decreased. In the AuNTs-PC electrode, the R_{ct} was decreased from 325 Ω to 93 Ω, table 2. The electric field amplified the ss-DNA sequences immobilization on the surface and increased the EIS response. Under the applied electrical potential force, the electric field compelled the DNA sequences to orientate and align in the preferred and favored direction, Fig. 5. By applying the electric field, the charge transfer was enhanced. This process supports the bio-sensing mechanism at very low concentrations. The applied electric field obligated the biosensor to operate and detect the HPV16 DNA in very low concentrations and high reproducibility.

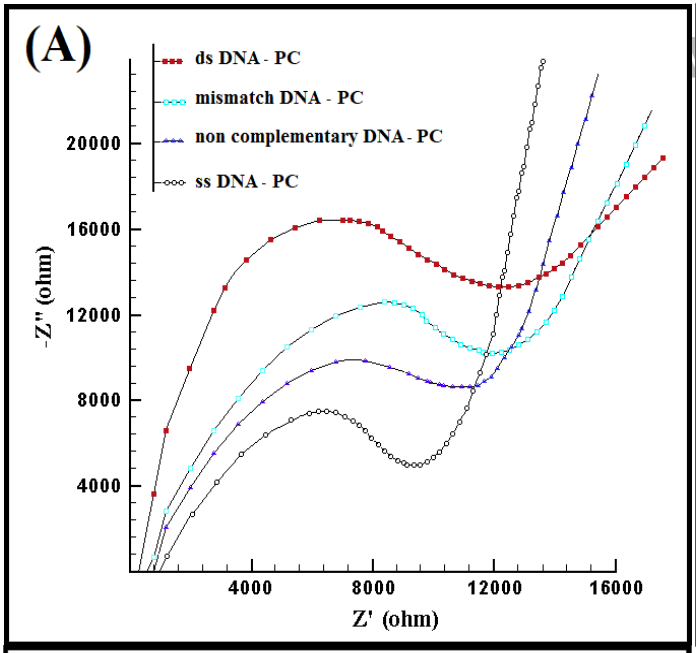
(A)
ds DNA - PC
mismatch DNA - PC
non complementary DNA - PC
ss DNA - PC
-Z'' (ohm)
Z' (ohm)
4000
8000
12000
16000
20000

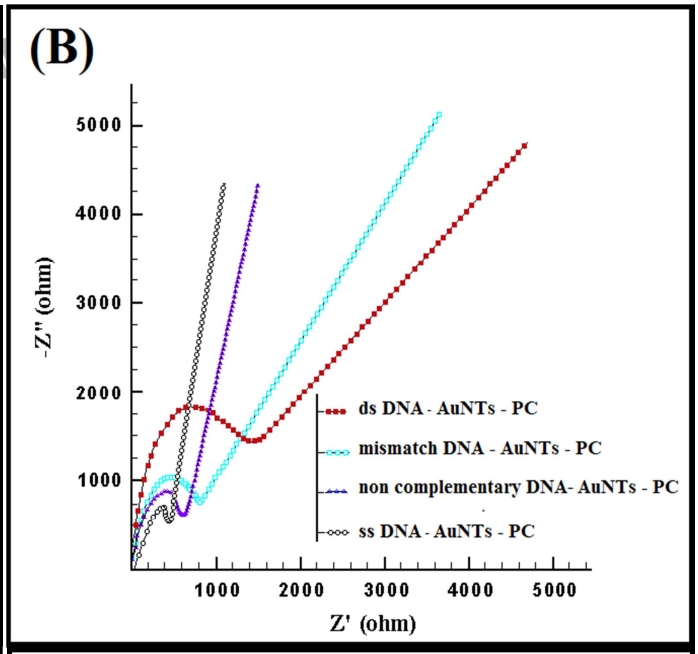
(B)
ds DNA - AuNTs - PC
mismatch DNA - AuNTs - PC
non complementary DNA- AuNTs - PC
ss DNA - AuNTs - PC
-Z'' (ohm)
Z' (ohm)
1000
2000
3000
4000
5000

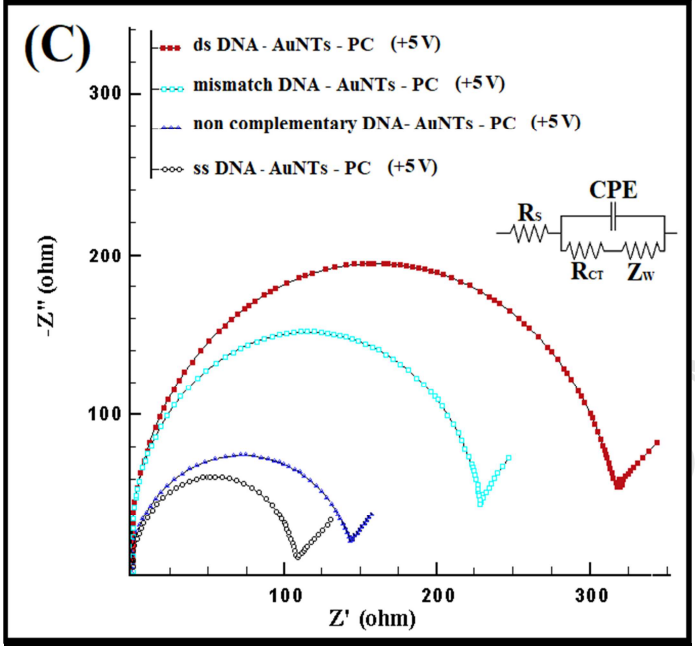
(C)
ds DNA - AuNTs - PC (+5 V)
mismatch DNA - AuNTs - PC (+5 V)
non complementary DNA- AuNTs - PC (+5 V)
ss DNA - AuNTs - PC (+5 V)
CPE
Rs
RCT
Zw
-Z'' (ohm)
Z' (ohm)
100
200
300

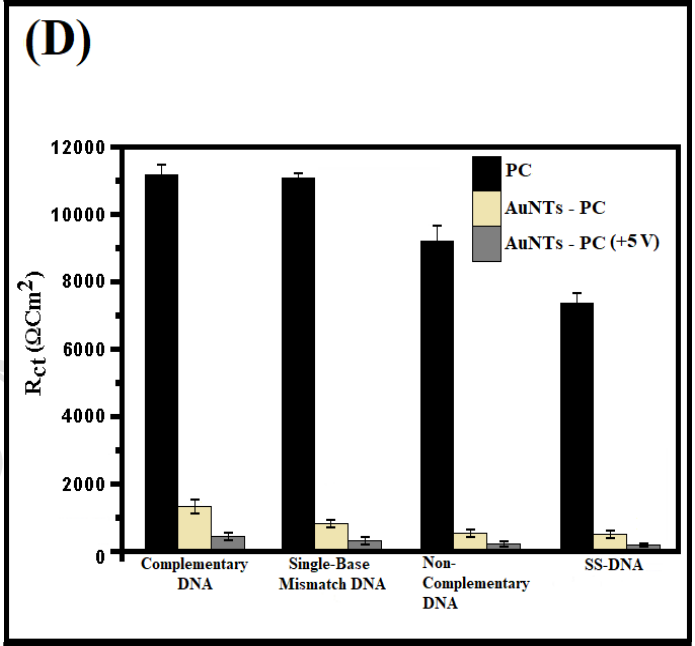
(D)
PC
AuNTs - PC
AuNTs - PC (+5 V)
Rct (ΩCm2)
Complementary DNA
Single-Base Mismatch DNA
Non-Complementary DNA
SS-DNA
0
2000
4000
6000
8000
10000
12000

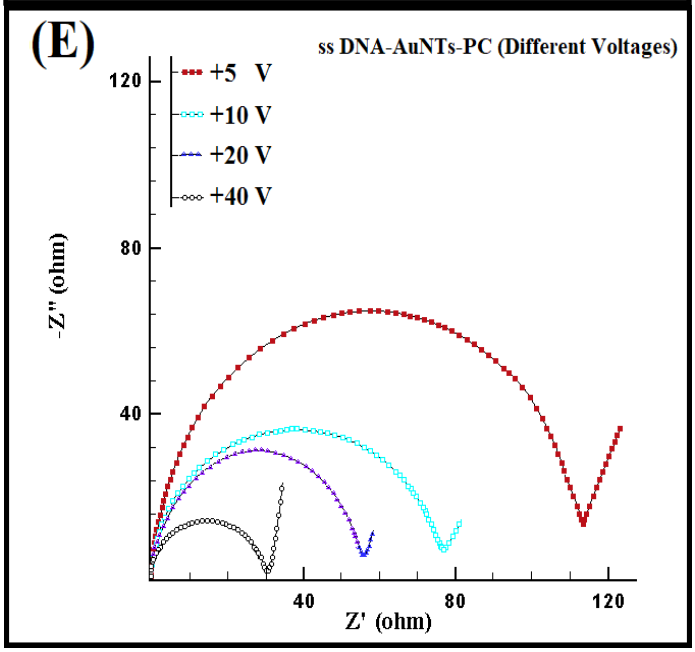
(E)
ss DNA-AuNTs-PC (Different Voltages)
+5 V
+10 V
+20 V
+40 V
-Z'' (ohm)
Z' (ohm)
40
80
120

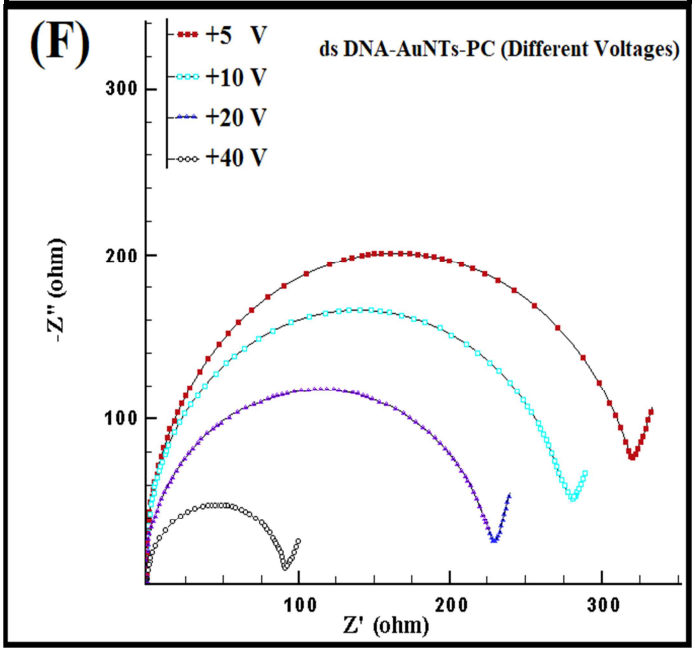
(F)
ds DNA-AuNTs-PC (Different Voltages)
+5 V
+10 V
+20 V
+40 V
-Z'' (ohm)
Z' (ohm)
100
200
300

Fig. 6. (A) The EIS impedance spectra of DNA oligonucleotides probe, mismatch, non-complementary and complementary target DNA oligonucleotides hybridization in the specificity test for PC electrode with 1 µM concentration. (B) The EIS impedance measurements of the probe, mismatch, non-complementary and complementary DNA oligonucleotides in the specificity test for AuNTs-PC electrode with 1 µM concentration. (C) The EIS impedance measurements of the probe, mismatch, non-complementary and complementary DNA oligonucleotides in the specificity test for AuNTs-PC electrode with 1 µM concentration under electric potential (+5 V). Inset; the simulated Randle's equivalent electrical circuit of the EIS biosensor. (D) The R_{ct} of bare PC and AuNTs-PC (with and without applying electric potential) electrodes modified with ss-DNA, non-complementary, mismatch and complementary DNA targets. All values in 1 µM concentration. (E) and (F) The electrochemical EIS plots of the probe immobilization and target hybridization for AuNTs-PC electrode under different electric potentials, respectively.

Table 2. The summary of the Randle's equivalent circuit parameters for the AuNTs-PC electrode under electric field amplification.

Sample	$R_S(\Omega)$	C_{DL} (µF)	N	$R_{CT}(\Omega)$	RSD Value	Z_W
ss-DNA (+5 V)	**6**	**0.000302**	**0.76**	**106**	**2.35%**	**0.0000497**
ss-DNA(+40 V)	**7**	**0.000361**	**0.81**	**26**	**2.07%**	**0.0000901**
ds-DNA(+5 V)	**14**	**0.000143**	**0.70**	**325**	**3.89%**	**0.0000264**
ds-DNA(+40 V)	**17**	**0.000202**	**0.84**	**93**	**1.93%**	**0.0000299**

3.2.2. The EIS responses, sensitivity and stability of the AuNTs-PC electrode (with and without electric potential)

The sensitivity and stability of the AuNTs-PC electrode responses with and without electric potential amplification were investigated. The sensitivity measurements were conducted by the examination of the biosensor response to various concentrations of the complementary target DNA oligonucleotides. The sensitivity of biosensor to the complementary sequences was measured for AuNTs-PC electrode (without electric potential) from 1 nM to 0.1 pM and with electric potential from 1 µM to 0.01 pM, Fig. 7A and Fig. 7B, respectively. The applying electric field helped the biosensor to reach the lower concentrations in comparison to non-existence electric field situation. It is important to note, due to weak immobilization and hybridization of DNA with the bare PC surface, the sensitivity of the bare PC electrode was ceased at 0.1 µM concentration and no significant sensitivity was achieved at lower concentrations.

The sensitivity of the AuNTs-PC electrode under electric potential reached to 0.01 pM. The R_{ct} values were increased with the enhancement in concentration of the complementary DNA target. In Fig. 7A and 7B, it is completely obvious that AuNTs-PC electrode indicated high sensitivity. Fig. 7C demonstrates the calibration curve for the hybridization of the probe with complementary HPV16 DNA target in different concentrations for the AuNTs-PC electrode under electric potential amplification. The calibration curve was plotted by the R_{ct} values achieved from the simulated Randle's equivalent electrical circuit of the EIS biosensor. Fig. 7C indicates that the changes in R_{ct} have a linear relationship with the log scale of complementary DNA sequences concentrations in the range from 1 µM to 0.01 pM in AuNTs-PC electrode, (Fig. 7C red line). The info-diagram clearly shows a high sensitivity of the AuNTs-PC electrode. In this case, the detection limit of 1 fM can be evaluated for AuNTs-PC electrode under electric potential, [2]. The LOD (limit of detection) was estimated via Eq. (2):

$$Y = S_b + 3\,\sigma_b \quad (2)$$

Where S_b is the signal of blank and σ_b is the standard deviation of blank.

The stability of the HPV biosensor was investigated after six weeks of storing the biosensor in the freezer at 4^oC, Fig. 7C (blue line). The results demonstrated that the maximum response of the biosensor

under external electrical potential force was able to retain 97% of its initial response after six weeks. This indicates that the fabricated electrochemical biosensor responses had longstanding stability.

Fig. 7D shows the calibration curve for the hybridization of the probe with complementary target in different concentrations for the AuNTs-PC biosensor without electric potential amplification. Fig. 7D indicates the effect of electric potential on the biosensor performance. The stability of the bare PC and AuNTs-PC electrodes (without electric potential) was also investigated after six weeks of storing the biosensors in the freezer at 4°C, and the results demonstrated that the maximum response of the bare PC and AuNTs-PC (without electric potential) biosensors were able to retain 32% and 91% of their initial responses, respectively. This proved that the AuNTs-PC electrode biosensor responses with and without electrical amplification have longstanding stability.

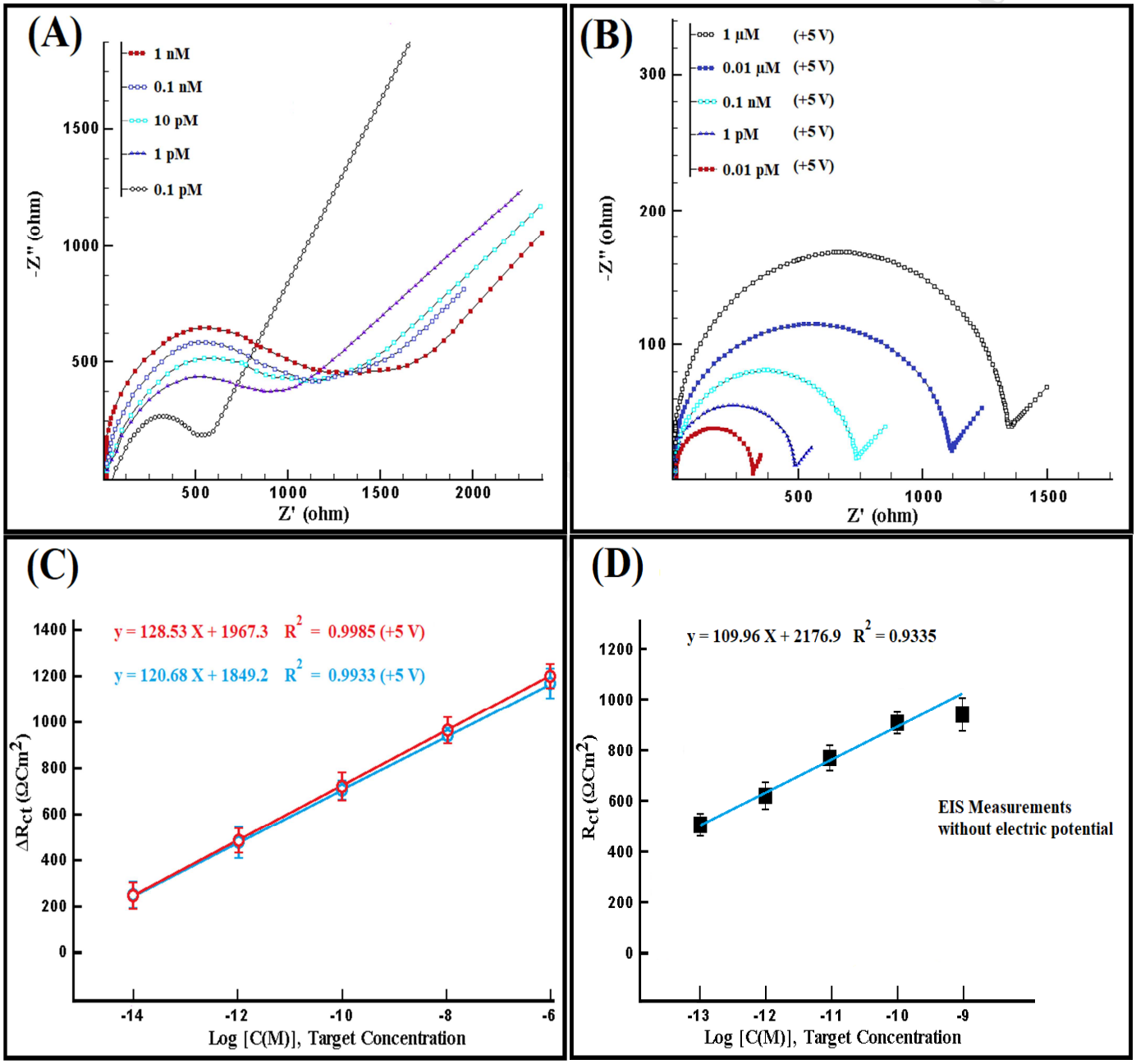

Fig. 7. The sensitivity of the AuNTs-PC electrode. (A) The sensitivity of biosensor to the complementary sequences for AuNTs-PC without electric potential, from 1 nM to 0.1 pM. (B) The sensitivity of biosensor to the complementary sequences for AuNTs-PC with electric potential (+5 V), from 1 µM to 0.01 pM. (C) The linear relation between the ΔR_{ct} and the log scale (log [C(M)]) of complementary DNA sequences concentrations in the AuNTs-PC electrode under electric potential amplification, (red line). The R_{ct} values derived from Randle's circuit. The stability of the AuNTs-PC DNA biosensor under electric potential (+5 V) after six weeks (blue line). (D) The R_{CT} vs. complementary target concentrations (log [C(M)]) for AuNTs-PC without electric potential, R_{CT} values derived from Randle's circuit.

3.2.3. Reproducibility of the bare PC and AuNTs-PC (with and without electric potential) electrodes

The investigation of the reproducibility of the fabricated DNA biosensors for both AuNTs-PC and PC electrodes in HPV16 bio-sensing after recording the measured data from three independent electrodes fixed in 1 µM concentration, was conducted. The relative standard deviations (RSD) values for AuNTs-PC without electric potential were 0.93, 3.77 and 4.76% for non-complementary, mismatch and complementary targets, respectively. While the RSD values for AuNTs-PC with electric potential (+5 V) were 0.88, 3.06 and 3.89% for non-complementary, mismatch and complementary targets, respectively. The RSD values lower than 9% indicate that the AuNTs-PC electrode has excellent reproducibility in bio-sensing diagnosis in comparison to previous reports, [2]. The RSD measured values for the bare PC electrode were 9.27, 12.1 and 13.53% for three types of the chosen targets, respectively. The weak reproducibility for the bare PC electrode has been achieved.

3.2.4. The surface coverage of the different electrodes

The surface coverage is related to the ratio of the target sequences hybridized with probe oligonucleotides on surface of the bio-electrode in certain concentrations, [24-29]. The surface coverage (Θ) can be calculated via Eq. (3):

$$\Theta = 1 - \frac{R_0}{R_i} \tag{3}$$

Where, R_0 is the charge transfer resistance obtained for ss-DNA bio-electrode and R_i is the charge transfer resistance obtained for ds-DNA bio-electrode for the specific target DNA concentrations. Fig. 8 indicates the surface coverage (Θ) of the PC and AuNTs-PC electrodes in different situations. It is obviously seen that the AuNTs-PC electrode under electrical field demonstrates more surface coverage in comparison to other electrodes even in lower concentrations. The most surface coverage was achieved by AuNTs-PC electrode under electrical field at +40 V interestingly in the lowest concentration (0.01 pM). In this situation, AuNTs-PC shows a maximum of 73.2% for probe on the surface being successfully hybridized with the complementary sequences.

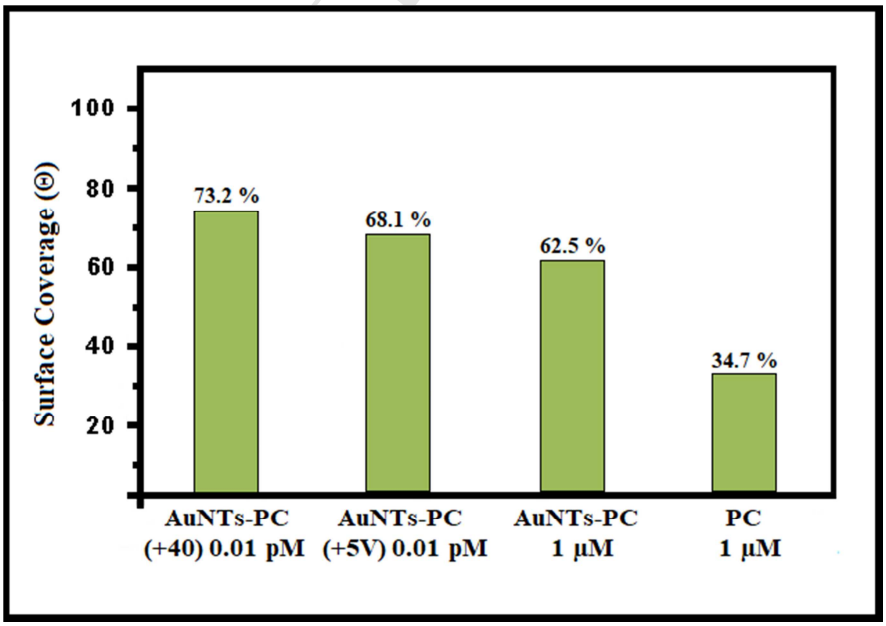

Fig. 8. The surface coverage of the different electrodes.

3. 3. Comparative study

Table 3 discusses the comparison of the recently published works on the HPV DNA bio-sensing with our work. The electrochemical biosensors were based on the label and the label free approaches. As shown in table 3, our proposed biosensor demonstrated a low LOD and a wide linear range that is comparable to the mentioned biosensors. This is due to the high sensitivity of the AuNTs surface. The AuNTs decorated PC could amplify the EIS signal under applied electrical field and enhance the detection response and sensitivity to the HPV DNA sequences.

Table 3. Comparison of the different biosensors for HPV detection

Biosensor Electrode	Linear Range	Detection Limit	Detection Technique	Reference
Au electrode/L-cysteine	18–250 nM	18 nM	DPV	[8]
Au electrode	0.1–50 nM	110 pM	Steps and Sweeps	[32]
Screen-printed Au electrode	0–770 pM.	0.308 pM	SWV	[5]
Au electrode	12.5 nM−350 nM	3.8 nM	CVand DPV	[6]
(Polyaniline-CNT) Platinum electrode	10 nM −50 nM	490 pM	CVand SWV	[7]
SWCNT/Au NPs	1 aM-1 µM	1 aM (Atto molar)	EIS	[4]
Carbon nano-nion modified GC	0–20 nM	0.5 nM	Amperometry	[3]
GC-GNS electrode	1 pM-1 µM	0.15 pM	EIS	[2]
AuNTs PC	0.01 pM-1 µM	1 fM	EIS	This Work

4. Conclusion

In this study, we have successfully designed and fabricated a high sensitive HPV16 DNA biosensor in label free detection based on AuNTs. The AuNTs-PC electrode accomplished the DNA hybridization detection in very low concentration and the EIS amplified signals were intensified by AuNTs and external electric field bias in order to acquire very low LOD in a wide linear detection range. Moreover, this novel bio-sensing electrode (DNA biosensor) could distinguish the complementary sequences from the mismatch and non-complementary oligonucleotides, indicating very good stability and maintenance. In conclusion, the materialized novel conceptual design and performance of the fabricated biosensor would be very attractive for human papilloma virus diagnosis and its genetic mutations.

5. References

[1] Van Ranst M, Kaplan JB, Burk RD (1992) Phylogenetic classification of human papillomaviruses: correlation with clinical manifestations. J Gen Virol 73(10):2653–2660

[2] Karimizefreh A, Aghakhani Mahyari F, VaezJalali M, Mohammadpour R, Sasanpour P (2017) Impedimetic biosensor for the DNA of the human papilloma virus based on the use of Au nanosheets. Microchimica Acta 184 (6): 1729–1737.

[3] Bartolome JP, Echegoyen L, Fragoso A (2015) Reactive carbon Nano-onion modified glassy carbon surfaces as DNA sensors for human papillomavirus oncogene detection with enhanced sensitivity. Anal Chem 87(13):6744–6751.

[4] Wang S, Li L, Jin H, Yang T, Bao W, Huang S, Wang J (2013) Electrochemical detection of hepatitis B and papilloma virus DNAs using SWCNT array coated with Au nanotubes. Biosens Bioelectron 41:205–210.

[5] Zari N,Amine A, Ennaji MM (2009) Label-free DNA biosensor for electrochemical detection of short DNA sequences related to human papilloma virus. Anal Lett 42(3):519–535.

[6] Nasirizadeh N, Zare HR, Pournaghi-Azar MH, Hejazi MS (2011) Introduction of hematoxylin as an electroactive label for DNA biosensors and its employment in detection of target DNA sequence and single-base mismatch in human papilloma virus corresponding to oligonucleotide. Biosens Bioelectron 26(5):2638–2644.

[7] Tran LD, Nguyen DT, Nguyen BH, Do QP, Le Nguyen H (2011) Development of interdigitated arrays coated with functional polyaniline/MWCNT for electrochemical biodetection: application for human papilloma virus. Talanta 85(3):1560–1565.

[8] Campos-Ferreira DS, Nascimento GA, Souza EVM, Souto-Maior MA, Arruda MS, Zanforlin DML, Ekert MHF, Bruneska D, Lima- Filho JL (2013) Electrochemical DNA biosensor for human papilloma virus 16 detection in real samples. Anal Chim Acta 804:258–263.

[9] Kang B, Yeo U, Yoo KH, (2010) Anodized aluminum oxide-based capacitance sensors for the direct detection of DNA hybridization. Biosensors and Bioelectronics, 25; 1592–1596

[10] Kim YJ, Kim YJ, Jones JE, Li H, Yampara-Iquise H, Zheng G, Carson C A, Cooperstock M, Sherman M, Yu Q, (2013) Three-dimensional (3-D) microfluidic-channel-based DNA biosensor for ultra-sensitive electrochemical detection. Journal of Electroanalytical Chemistry, 702; 72–78

[11] Wu S, Ye WW, Yang M, Taghipoor M, Meissner R, Brugger J, Renaud P, (2015) Impedance sensing of DNA immobilization and hybridization by microfabricated polycarbonate nanopore templates. Sensors and Actuators B, 216; 105–112

[12] Santos A, Kumeria T, Losic D, (2013) Nanoporous anodic aluminum oxide for chemical sensing and biosensors. Trends in Analytical Chemistry, 44

[13] Rahman MM, Li XB, Lopa NS, Ahn SJ, Lee JJ (2015) Electrochemical DNA Hybridization Sensors Based on Conducting Polymers. Sensors, 15; 3801-3829

[14] Ye W, Xu Y, Zheng L, Zhang Y, Yang M, Sun P (2016) A Nanoporous Polycarbonate Template Based Electrochemical Biosensor for Histamine Determination with Biofunctionalized Magnetic Nanotubes Concentration and Signal Amplification. Sensors, 16; 1767

[15] Bonanni A, PividoriMI, del ValleM (2010) Impedimetric detection of influenza a (H1N1) DNA sequence using carbon nanotubes platform and Au nanotubes amplification. Analyst 135(7):1765– 1772.

[16] Yang G, Chen Y, Li L, Yang Y(2011) Direct electrochemical determination of morphine on a novel Au nanotube arrays electrode. Clinica Chimica Acta 412: 1544

[17] Wang Y, Zhu Y, Liu Y, Yang Y, Ruan Q, Xu F (2010) An effective Au nanotubes electrode for amperometric biosensor. J Nanosci Nanotechnol. 10 (12); 8286-92

[18] Torati SR, Reddy V, Yoon SS, Kim C (2016) Electrochemical biosensor for Mycobacterium tuberculosis DNA detection based on Au nanotubes array electrode platform; Biosens Bioelectron. 15(78):483-8

[19] Zhang Z, Ma C, He L, Zhu S, Hao X, Xie W, Zhang W, Zhang Y (2014) Ultrafast synthesis of Au(I)-dodecanethiolate nanotubes for advanced Hg2+ sensor electrodes", Nanoscale Research Letters 9: 601

[20] Siwy Z, Trofin L, Kohli P, Baker L A, Trautmann C, and Martin C R (2005) Protein Biosensors Based on Biofunctionalized Conical Au Nanotubes; J. Am. Chem. Soc. 127(14): 5000–5001

[21] Kim Y J, Jones J E, Li H, Yampara-Iquise H, Zheng G, Carson C A, Cooperstock M, Sherman M, Yu Q (2013) Three-dimensional (3-D) microfluidic-channel-based DNA biosensor for ultra-sensitive electrochemical detection; Journal of Electroanalytical Chemistry 702: 72–78

[22] McPhillips J, Murphy A, Jonsson M P, Hendren W R, Atkinson R, Höök F, Zayats A V and Pollard R J (2010) High-Performance Biosensing Using Arrays of Plasmonic Nanotubes ACS Nano 4 (4): 2210–2216.

[23] Bianchini C, Zane D, Curulli A (2015) Au microtubes assembling architecture for an impedimetric glucose biosensing system, Sensors and Actuators B: Chemical, 220: 734-742

[24] Krishnamoorthy K., Zoski C. G(2005) Fabrication of 3D Au Nanoelectrode Ensembles by Chemical Etching; Analytical Chemistry 77: 5068

[25] Bahari Mollamahalle Y, Ghorbani M, Dolati A (2012) Electrodeposition of long Au nanotubes in polycarbonate templates as highly sensitive 3D nanoelectrode ensembles, Electrochimica Acta 75: 157–163

[26] Su H, Surrey S, McKenzie S, Fortina P, Graves D (2002) Kinetics of heterogeneous hybridization on indium tin oxide surfaces with and without an applied potential, Electrophoresis 23 :1551-1557

[27] Novelli G, Gennarelli M, Potenza L, Angeloni P, Dallapiccola B (1991) Study of the effects on DNA of electromagnetic fields using clamped homogeneous electric field gel electrophoresis, Biomedicine & Pharmacotherapy 45: 451-454

[28] Asbury C, van den Engh G, (1998) Trapping of DNA in Nonuniform Oscillating Electric Fields , Biophysical Journal 74: 1024–1030.

[29] Gokce Z G, Akalın P, Kok NF, Sarac AS (2018) Impedimetric DNA biosensor based onpolyurethane/poly(m-anthranilic acid) nanofibers; Sensors and Actuators B 254; 719–726

[30] Tak M, Gupta V, Tomar M (2017) an electrochemical DNA biosensor based on Ni doped ZnO thin film for meningitis detection. Journal of Electroanalytical Chemistry 792: 8–14.

[31] Torati S Ru, Reddy V, Yoon SS, Kim CheolGi (2016) Electrochemical biosensor for Mycobacterium tuberculosis DNA detection based on Au nanotubes array electrode platform. Biosensors and Bioelectronics 78: 483-488

[32] Civit L, Fragoso A, Hölters S, Dürst M, O'Sullivan CK (2012) Electrochemical genosensor array for the simultaneous detection of multiple high-risk human papilloma virus sequences in clinical samples. Anal Chim Acta 715:93–98

Highlights

*Impedimetric human papillomavirus DNA biosensor by AuNTs-PC electrode was fabricated

*The EIS response was intensified by AuNTs and electric field to acquire LOD of 1fM

*Biosensor in label free detection showed the good linear ranges of 0.01pM to 1μM

*Biosensor could highly specify ds-DNA from the mismatch and non-complementary targets

*Biosensor was stable up to 6 weeks and showed 97% of its initial detection responses